EEG Electrode Sensitivity—An Application of Reciprocity

STANLEY RUSH, SENIOR MEMBER, IEEE, AND DANIEL A. DRISCOLL, STUDENT MEMBER, IEEE

Abstract—**In this paper, the reciprocity theorem is used to determine the sensitivity of EEG leads to the location and orientation of sources in the brain. Quantitative information used in determining the sensitivity is derived from constant potential plots of a three-concentric-sphere mathematical model of the head with current applied through surface leads (the reciprocal problem), and from an electrolytic tank employing a human skull. Advantages of the reciprocal or lead field approach are outlined and the following conclusions are drawn. 1) Leads placed at the end of a diameter through the center of the brain have a range of sensitivity due to source location of only 3 to 1. 2) For the same electrode placement, sensitivity is maximum to sources oriented parallel to the line of the electrodes regardless of source location. 3) Electrodes spaced 5 cm apart are about ten times more sensitive to proximal cortical sources (by virtue of position) than to sources near the center of the brain.**

In the Appendixes, the solution is derived for the potential and current density in three concentric conducting spheres energized by arbitrarily placed point electrodes on the surface, and the reciprocity theorem is extended to inhomogeneous anisotropic media.

Introduction

In A recent paper, we published quantitative details of the current distribution in the brain resulting from the application of current-carrying electrodes to the surface of the head [1], there being several areas of medicine in which electrical currents are so employed. It was shown that for many applications it is sufficient to model the head mathematically as three concentric spheres. Thus, information about current flow in the head can be obtained from mathematical equations containing the individual's geometrical and electrical characteristics.

In this paper, by means of the reciprocity theorem, we reinterpret the data to describe, again quantitatively, how a given EEG lead will respond to sources within the brain, and how the effect of variations in head size, skull and scalp thickness, and tissue resistivity may be calculated. The theory thus provides the physical foundation for a more scientific interpretation of the EEG and serves as a starting point for the rational synthesis of optimal lead arrays for specific purposes.

Direct studies of the relationship of the brain source to the surface lead, correlated with mathematical models, have been made by Brazier (homogeneous model) [2], Geisler and Gerstein (two concentric spheres) [3], and more recently by Paicer, Sances, and Larson (three concentric spheres) [4]. The data to be given here are based on a similar three-concentric-sphere mathematical model, but on different experimental techniques, the interpretation of which is founded on the reciprocity theorem. The reciprocity approach has a considerable conceptual and practical advantage as has been established in electrocardiography.

The remainder of this paper is arranged in the following fashion. The next section gives a brief review of the principles of reciprocity and a theoretical example which compares surface potentials obtained directly with those obtained by reciprocity. The section following discusses briefly the methods used to establish the validity of the three-sphere model. The next and principal section shows the basic lead field information and discusses the conclusions about the sensitivity of surface leads which can be drawn from the data. Appendix I extends the reciprocity theorem to anisotropic media; Appendix II outlines the method of solution and gives the resulting expressions for the fields due to point current sources on the outer surface of three concentric spheres.

Reciprocity

The reciprocity theorem was first introduced into biophysical areas in 1853 by Helmholtz [5], and its modern usage in electrocardiography is due to the vision of Dr. Frank Wilson. As a result of the latter's interest, important papers on this subject were published by his colleagues McFee and Johnston [6] and by Brody and Romans [7]. Subsequently, the theory was developed in considerably more detail by Brody, Bradshaw, and Evans [8] and by Plonsey [9].

Brain, among other body tissues, is known to be anisotropic [10]. It follows that the use of any theorem in the interpretation of electrical signals from the brain presupposes that the theorem is applicable to anisotropic media. The use of reciprocity here has therefore been justified by an extension in Appendix I of Plonsey's [9] proof of the theorem.

In many cases it is possible to approximate an anisotropic medium as alternating layers of high- and lower-resistivity isotropic material. [11] From this point of view, the established reciprocity theorems for inhomogeneous media may be considered suitable for the anisotropic situation. Here we review and integrate the subject of reciprocity at a practical level for the reader interested in biological applications. The discussion will also serve as a basis for the succeeding developments.

First, we consider the source of the EEG in terms of its appropriate mathematical description. The electrical

Manuscript received January 24, 1968; revised July 1, 1968. This work was supported by a NASA Sustaining Grant.

The authors are with the Department of Electrical Engineering, University of Vermont, Burlington, Vt.

effects measured at the body surface arise from the disturbance of the uniform double layers of charge surrounding excitable cells. These cells in their resting state have the property of being "electrically silent"; that is, they produce no electrical forces either inside or outside the cell. The closed double layer is manifested by a change from zero potential to the resting potential as an exploring probe crosses the membrane. A partial breakdown of this specialized charge arrangement results in the exposure of the surrounding tissue to electrical forces and, hence, current flow. Current flow from such an active region tends to appear as if it came from a positive and a negative source separated by a small distance, that is, a dipole source.

As a practical matter, it has been customary (particularly in the electrocardiographic literature) to treat a small block of tissue containing excitable cells as a dipole source in a locally homogeneous environment. The strength and orientation of each dipole may vary with time, and the total effect at a remote point is considered as the superposition of the individual effects. The precise relationship of each effective dipole to the individual cells and their transmembrane potentials has not yet been established and will not be considered further here.

Before discussing the reciprocity theorem itself, it is necessary to consider the mathematical description of the dipole source. Helmholtz, and also McFee and Johnston, considered the dipole as an element of a double layer of charge (an electromotive surface). This element has an area A and a potential difference across it e. It is conveniently described by a vector $\overline{Ae}$, having a magnitude equal to Ae, direction perpendicular to A, and pointing from the negative to the positive side. A second, more conventional description, was introduced by Brody and Romans. In it, the dipole is considered a point source of current i and a sink $-i$ spaced a small distance D apart. Again the dipole can be given a vectorial description $\overline{iD}$.

Helmholtz's statement of reciprocity considered two elements of electromotive surface $\overline{e_mA_m}$ and $\overline{e_nA_n}$ activated one at a time. Define i_{nm} as the current through area A_n due to $\overline{e_mA_m}$ when $e_n=0$ and i_{mn} as the current through area A_m due to $\overline{e_nA_n}$ when $e_m=0$. Helmholtz proves that

$$\frac{e_mA_m}{i_{nm}} = \frac{e_nA_n}{i_{mn}}.$$

This statement of reciprocity can then be applied, using superposition (linearity is assumed in the proof), to arbitrary combinations of electromotive surfaces.

As noted above, Helmholtz's theorem has been extended and rederived in several ways. We consider here two specializations which are of interest.

Assume a volume conductor with an active dipolar source in the interior at point P and two points α and β on the surface between which a potential difference $V_{\alpha\beta}$ is measured. Assume a second case with the identical volume conductor in which the interior source is deactivated and a current $I_{\alpha\beta}$ is introduced through points α and β, and a current density $\overline{J}$ is measured at P.

The McFee-Johnston statement of reciprocity then reads

$$V_{\alpha\beta} = (\overline{J}/I_{\alpha\beta})\cdot\overline{eA}. \tag{1}$$

The quantity $(\overline{J}/I_{\alpha\beta})$ is the current density per ampere applied and is called the "lead field"; its value at the point P is called the "lead vector". $V_{\alpha\beta}$ is the lead voltage (potential difference) due to the dipole $\overline{eA}$. $I_{\alpha\beta}$ and e are nonzero at different times in accordance with the conditions of the previous paragraphs.

The Brody-Romans statement with the dipole described as iD is given as

$$V_{\alpha\beta} = (\overline{E}/I_{\alpha\beta})\cdot\overline{iD}. \tag{2}$$

The quantity $(\overline{E}/I_{\alpha\beta})$ is the electric intensity per ampere applied, and its value at the location P of the current dipole is also called the lead vector.

Thus, because of the different choices of source units, the lead vectors have correspondingly different units. The difference is only a matter of a constant, however, which can be attributed to the conductivity σ at the dipole location. Thus, since $\overline{J}=\sigma\overline{E}$, (1) and (2) will give identical results if $(\overline{iD}/\sigma)$ is assumed equal to $\overline{eA}$. Since we are usually interested in the *relative* effects of the internal sources, the above factors are normally not considered.

The reciprocity method, then, using the notation of (1), is the following. Given a dipole (equivalent) source $\overline{eA}$ and a need to know the resulting potential difference $V_{\alpha\beta}$ between two points α and β, (1) shows that it suffices to find the current density at the dipole location resulting from a unit current through points α and β. Similarly, from (2), it is sufficient to find the electric intensity at the dipole location. Current density and electric intensity are obtained easily from an equipotential field plot.

There are distinct advantages to the reciprocity approach. As will be seen, a single display of the constant potentials from current introduced through surface leads gives a complete picture of the sensitivity of those leads to the location and direction of internal sources. It is also relatively easy to visualize intuitively the approximate effects of inhomogeneities and of lead position changes on current flow patterns. An additional major advantage has to do with the practical problems of instrumentation for artificial "source–surface" measurements *in vivo* or in an electrolytic tank. It is usually convenient and sufficiently accurate to use fairly large electrodes on the surface, but it is desirable to use small electrodes where the sources are located. Correspondingly, as is required in the lead field instrumentation, it is easy to put large currents through large electrodes and to measure potential through small electrodes.

These ideas can be illustrated by an example relevant to EEG and electroanesthesia (EA) studies. Consider a current dipole element of strength $\overline{iD}$ at the origin of three concentric spheres (representing the head). The potential distribution Φ in the outer layer (scalp) is obtained by conventional procedures as

$$\Phi(r, \theta) = \frac{A_1}{6\pi\sigma_t c^2}\left[2\frac{r}{c} + \left(\frac{c}{r}\right)^2\right] iD \cos\theta. \quad (3)$$

The constants A_1, σ_t, and c are defined in Appendix II. The potential difference $V_{\alpha\beta}$ between a lead pair placed at the poles on the surface is found from (3) as

$$V_{\alpha\beta} = 2\Phi(c, 0) = \frac{A_1}{\pi\sigma_t c^2} iD. \quad (4)$$

From the solution of the reciprocal problem [Appendix II, (30)] for current $I_{\alpha\beta}$ applied to the same lead pair, the electric intensity at the origin per ampere applied E/I is

$$E/I_{\alpha\beta} = -\frac{J_b}{\sigma_b I_{\alpha\beta}} = \frac{A_1}{\pi\sigma_t c^2}. \quad (5)$$

Substitution of this expression for $E/I_{\alpha\beta}$ into (2) is seen to give the same result for $V_{\alpha\beta}$ as appears in (4), thereby satisfying the reciprocity theorem.

Validity of the Three-Sphere Model

It has been shown in an earlier paper [1] that a three-sphere (brain, skull, scalp) model of the head is a useful representation for many purposes. The data from the model have been compared to electrolytic tank measurements employing a human skull, to *in vivo* data from within a monkey brain, and to *in vivo* data taken from the surface of the head. With some minor exceptions (the reasons for which are explained), the correlations are such as to indicate clearly that the model has adequate accuracy for most purposes presently foreseen. One example showing the data comparisons is given in the next section.

Sensitivity of Surface Leads to Source Location

The principal objective of this paper is to provide useful information, for a typical human head, about the sensitivity of surface leads to source location and orientation. To this end we show several potential plots from surface lead connections to different parts of the head. Fig. 1 shows the computed data for four different lead connections, but with otherwise common dimensions and electrical parameters. Since the symmetry of a sphere is such as to make various orientations indistinguishable, these plots apply to all lead pairs with the indicated spacing regardless of the actual position on the surface of the head. The equations in Appendix II show the method for introducing arbitrary sphere radii and resistivities. Fig. 3 is an adaptation of the data of Fig. 1(a) scaled to fit the electrolytic tank data of Fig. 2. Figs. 2 and 3 are included for the comparison of experimental and theoretical measurements, and to demonstrate the modification of Fig. 1 required for specific applications. The scaling of Fig. 1(a) involved decreasing the potentials and current densities by a factor of 500 due to the decrease in applied current (from 1 mA to 2 μA), and increasing the potentials by another factor of 10 due to the increase in resistivity (from 222 to 2220 $\Omega\cdot$cm). Current density is affected by changes in resistivity ratios, but not by a scaling of all resistivities. The current density at every point is directly proportional to the total current through the electrodes, the relative densities remaining the same throughout.

The lead field has a direction perpendicular to the equipotential lines and an intensity inversely proportional to their spacing. Thus the lead fields can easily be visualized and an overall grasp of the lead sensitivity obtained. A few current density values at points under the electrodes, at the vertex and at the brain center, are also shown on the figures. In interpreting the plots, it is necessary to note that the sensitivity of the leads is maximum to the dipolar sources oriented in the direction of the lead field (perpendicular to the equipotential lines), and falls off as the cosine of the angle between the source and lead field directions.

As examples of the use of the data, several specific conclusions from Fig. 1 will be mentioned. In all cases, there is, by virtue of the symmetry, a constant potential plane surface (shown as a straight line) through the brain center. No sources, or components of the sources, parallel to and lying in this plane will be detected by the given electrodes. The current density at the center varies from 3.7 μA/cm^2 in Fig. 1(a) to 0.96 μA/cm^2 in Fig. 1(d) as the electrodes approach the vertex from the 0°–180° positions. Thus, the closely spaced electrodes are approximately one-fourth as sensitive to sources at the center, assuming they have a common orientation, as are electrodes along the diameter. In the cortex midway between the electrodes, the current densities range from 2.8 μA/cm^2 to 8.8 μA/cm^2 as the electrodes are brought closer together, forming a 3-to-1 ratio. Thus the greater sensitivity to sources at this point occurs when the electrodes are about 5 cm apart. Looking again at Fig. 1(d), it can be seen that the constant potentials in the cortex in the 75°–85° region are somewhat more closely spaced and differently oriented than they are at the brain vertex at the same radius. Thus, the midline is not the source location to which the electrodes are most sensitive, although the difference due to position (rather than orientation) is not great.

Detailed information thus can be derived from the figures, but some interesting generalizations can also be deduced. In Fig. 1(a), or equivalently in Figs. 2 or 3, in which the EEG electrodes are placed at the front and back of the head, it can be seen that this lead pair is almost equally sensitive to sources anywhere in the entire brain. The range of sensitivities to sources in the cortex

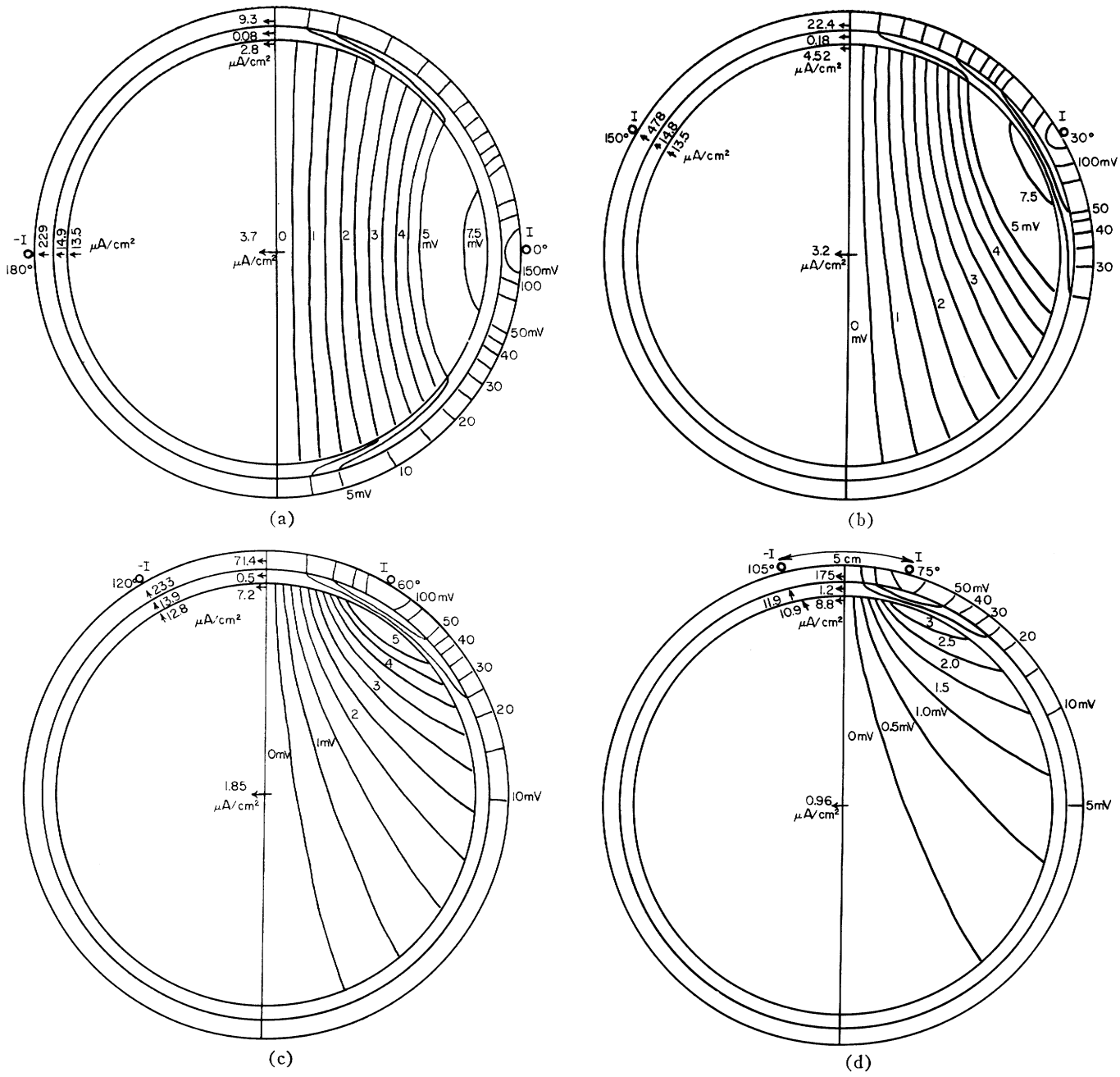

Fig. 1. Theoretical data from the three-sphere model. Potential plots are shown from four electrode positions: (a) at 0° and 180°, (b) at 30° and 150°, (c) at 60° and 120°, and (d) at 75° and 115°. Since the configuration is symmetrical, potential data are shown only on the right-hand side. Current density vectors are shown on the left at key positions: center, vertex (brain, skull, and scalp), and maximum (in brain, skull, and scalp under electrode). $I=1$ mA; skull resistivity is 80 times the 222 Ω·cm used for the brain and scalp; radii are 8.0, 8.5, and 9.2 cm.

immediately under the electrodes to a source at the brain center expressed as a ratio is only 2.5 to 1. This rises to only 3 to 1 when the second point is in the cortex midway between the electrodes where the current density is minimum. Also, for this electrode pair, the figure shows that the source directions for maximum sensitivity are essentially the same for all positions in the brain and that this direction is parallel to the line of the electrodes. Further, the above conclusions indicate that each of three such electrode pairs which lie along three mutually perpendicular lines will measure independent EEG information, i.e., data from one of the three vector components of the dipole sources. These are characteristics of "heart vector" leads used in vectorcardiography. Also, as in the heart, a significant amount of the electrical source activity may be of the form of closely spaced, but oppositely directed, dipoles. Such sources will be to a large degree self-cancelling so far as surface effects are concerned.

As was noted in our earlier paper [1], the resistivity of skull is quite variable. For this reason the change in sensitivity of a lead pair due to changing skull-brain resistivity ratio is of interest. Although the purpose of this paper is to present the method of calculation and

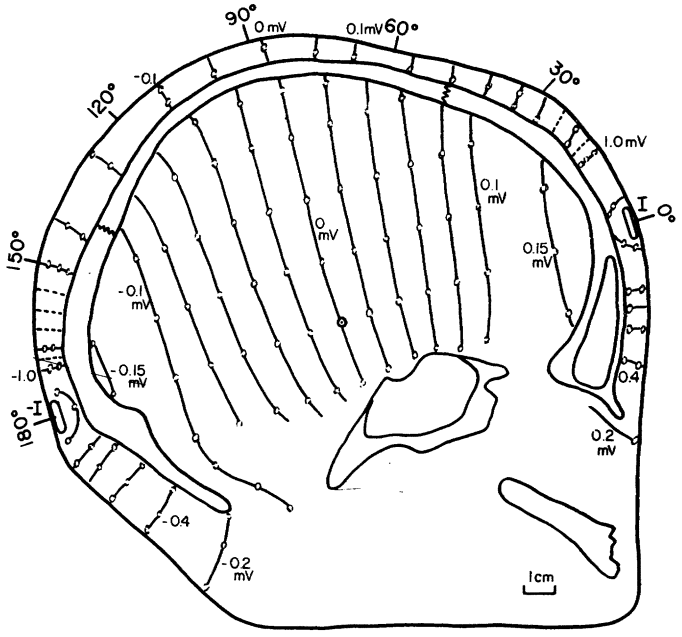

Fig. 2. Potential data at surface of electrolytic tank (midsagittal plane). Lines between 0.1-mV curves are spaced at equal potential differences (0.02 mV) apart. Electrodes at 0° and 180° are near centers of frontal and occipital bones, respectively. $I=1.0$ μA in the half-head model; fluid resistivity is 2220 Ω·cm.

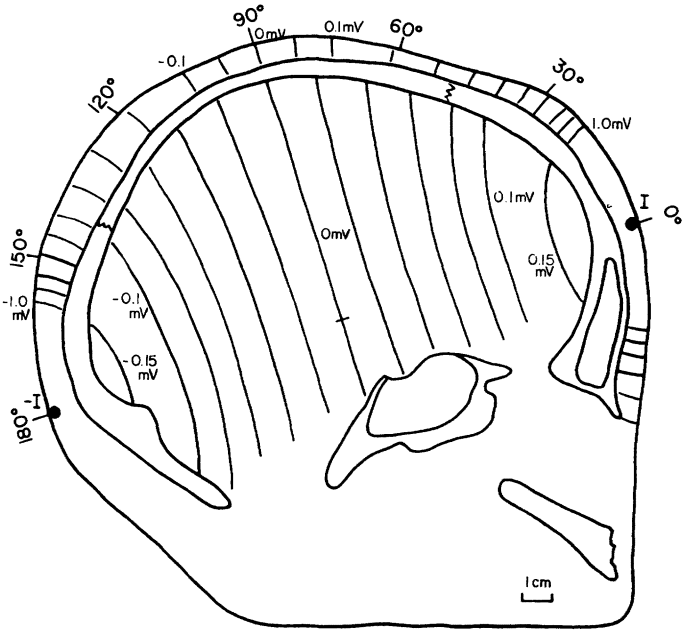

Fig. 3. Potential data from three-sphere model of Fig. 1 (a), scaled and presented in the same form as that obtained from the tank. The same constant potential lines are shown in the brain as in Fig. 2, but are computed from the three-sphere model. The radii are 8.0, 8.5, and 9.2 cm; the skull is assumed isotropic with a resistivity 80 times the 2220 Ω·cm of the fluid used in the scalp and brain regions of the electrolytic tank. $I=2$ μA in the sphere (equivalent to 1 μA in a half-sphere).

general results, rather than detailed and exhaustive data, an estimate of the effect of a change in this ratio is given here.

In the range of ratios 60 to 100 for the lead pair of Fig. 1(a) the sensitivity is very nearly a linear function of the resistivity ratio. The sensitivity to proximal cortical sources will decrease (increase) by 1 percent; the sensitivity to sources at the brain center will decrease (increase) by 1/2 percent; and the sensitivity to those at the brain vertex will decrease (increase) by 1/3 percent per unit increase (decrease) in the resistivity ratio from the value 80 used for Fig. 1(a). Thus, if the skull-brain resistivity ratio in Fig. 1(a) were changed to 70, the current density (lead field vector) at the brain center would become 3.9 μA/cm^2 (3.7 μA/cm^2 plus 5 percent of 3.7 μA/cm^2).

As shown in Fig. 1, the lead field strength and orientation become much more dependent on position in the brain as the electrodes are brought closer together. In these cases, a careful examination of the lead fields is required to interpret properly the sources which may be influencing the leads. Nevertheless, a significant result is that surface leads spaced 5 cm apart are approximately ten times more sensitive to proximal cortical sources (by virtue of position) than to sources in the center of the brain (with the same orientation). Closer lead spacings are relatively insensitive to brain activity due to the shunting effect of the scalp. The sensitivity to proximal cortical sources is increased (decreased) by 1 percent per unit decrease (increase) in the skull-brain resistivity ratio from the value 80 used in Fig. 1(d).

Summary

In this paper, we have employed potential and current density calculations in the brain resulting from surface electrodes to determine the sensitivity of EEG leads to source location and orientation. The reciprocity theorem is used as the theoretical basis for this method. The approach has the advantage of displaying the entire sensitivity relationship of a given lead pair in a simple figure. With only a few such equipotential plots, an overall grasp of the relationship of the brain source to the surface lead can be obtained. Most of the data presented are based on a three-sphere mathematical model of the head, the equations of which are derived in Appendix II. The accuracy and limitations of this model have been discussed in a companion paper [1].

Appendix I

Proof of the Reciprocity Theorem for the General Inhomogeneous Anisotropic Medium

Assume that for an arbitrary conductor

$$J^x = \sigma_{11}(x,y,z)E_x + \sigma_{12}(x,y,z)Ey + \sigma_{13}(x,y,z)E_z$$
$$J^y = \sigma_{21}(x,y,z)E_x + \sigma_{22}(x,y,z)Ey + \sigma_{23}(x,y,z)E_z$$
$$J^z = \sigma_{31}(x,y,z)Ex + \sigma_{32}(x,y,z)E_y + \sigma_{33}(x,y,z)E_z$$

in which $\sigma_{12}=\sigma_{21}$, $\sigma_{13}=\sigma_{31}$, and $\sigma_{23}=\sigma_{32}$. Then

$$J^i = \sigma^{ij}E_j \tag{6}$$

where σ^{ij} is a symmetrical tensor of rank 2. The electric field intensity E_j can be derived from the potential Φ as

$$E_j = -\nabla\Phi = -\Phi_{,j} \tag{7}$$

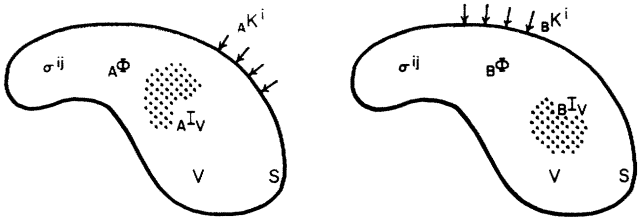

Fig. 4. Geometry for reciprocity theorem. (a) Case A. (b) Case B.

so that the current density becomes

$$J^i = -\sigma^{ij}\Phi_{,j}. \tag{8}$$

For volume current sources I_V we have from (8) that

$$I_V = \nabla\cdot J^i = J_{,i}{}^i = -\nabla\cdot(\sigma^{ij}\Phi_{,j}). \tag{9}$$

Consider the two cases A and B for the volume V of Fig. 4, where $_AI_V$ and $_BI_V$ are volume current sources, and $_AK^i$ and $_BK^i$ are surface densities of current flow into V across the boundary S. Then for case A

$$_AI_V = -\nabla\cdot(\sigma^{ij}{}_A\Phi_{,j}) \tag{10}$$

$$_AK_in_ids = (\sigma^{ij}{}_A\Phi_{,j})n_ids \tag{11}$$

and for case B

$$_BI_V = \nabla\cdot(\sigma^{ij}{}_B\Phi_{,j}) \tag{12}$$

$$_BK^in_ids = (\sigma^{ij}{}_B\Phi_{,j})n_ids \tag{13}$$

where n_i is the unit normal on S.

Beginning with the identity

$$\nabla\cdot(\Phi A^j) = (\Phi A^j)_{,j} = \Phi A^j{}_{,j} + \Phi_{,j}A^j$$

one obtains

$$\nabla\cdot{}_A\Phi(\sigma^{ij}{}_B\Phi_{,j}) = {}_A\Phi\nabla\cdot(\sigma^{ij}{}_B\Phi_{,j}) + {}_A\Phi_{,j}(\sigma^{ij}{}_B\Phi_{,j}) \tag{14}$$

$$\nabla\cdot{}_B\Phi(\sigma^{ij}{}_A\Phi_{,j}) = {}_B\Phi\nabla\cdot(\sigma^{ij}{}_A\Phi_{,j}) + {}_B\Phi_{,j}(\sigma^{ij}{}_A\Phi_{,j}). \tag{15}$$

Subtracting (15) from (14) results in

$$\nabla\cdot{}_A\Phi(\sigma^{ij}{}_B\Phi_{,j}) - \nabla\cdot{}_B\Phi(\sigma^{ij}{}_A\Phi_{,j}) = {}_A\Phi\nabla\cdot(\sigma^{ij}{}_B\Phi_{,j}) - {}_B\Phi\nabla\cdot(\sigma^{ij}{}_A\Phi_{,j}) \tag{16}$$

since, due to symmetry of σ^{ij},

$${}_A\Phi_{,j}(\sigma^{ij}{}_B\Phi_{,j}) = {}_B\Phi_{,j}\sigma^{ij}{}_A\Phi_{,j} = {}_B\Phi_{,j}(\sigma^{ji}{}_A\Phi_{,i}).$$

Integrating (16) over the volume V results in

$$\iiint_V \nabla\cdot{}_A\Phi(\sigma^{ij}{}_B\Phi_{,j})dV - \iiint_V \nabla\cdot{}_B\Phi(\sigma^{ij}{}_A\Phi_{,j})dV = \iiint_V {}_A\Phi\nabla\cdot(\sigma^{ij}{}_B\Phi_{,j})dV - \iiint_V {}_B\Phi\nabla\cdot(\sigma^{ij}{}_A\Phi_{,j})dV. \tag{17}$$

From the divergence theorem

$$\iiint_V A^i{}_{,j}dV = \iint_S A^in_jdS$$

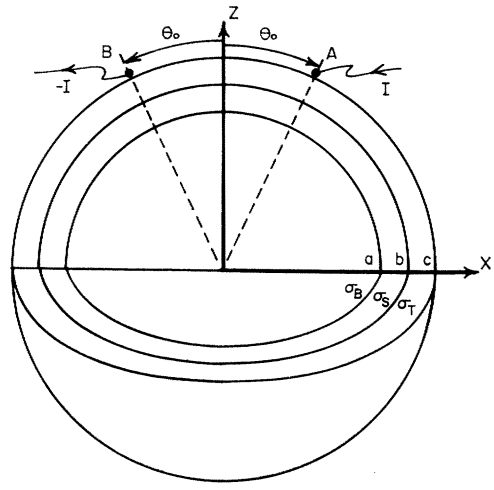

Fig. 5. Geometry for the three-concentric-sphere proof.

and (17) becomes

$$\iint_S {}_A\Phi(\sigma^{ij}{}_B\Phi_{,j})n_idS - \iint_S {}_B\Phi(\sigma^{ij}{}_A\Phi_{,j})n_idS = \iiint_V {}_A\Phi\nabla\cdot(\sigma^{ij}{}_B\Phi_{,j})dV - \iiint_V {}_B\Phi\nabla\cdot(\sigma^{ii}{}_A\Phi_{,j})dV. \tag{18}$$

Using (10)–(13), (18) becomes

$$\iint_S {}_A\Phi_BK^in_idS - \iint_S {}_B\Phi_AK^in_idS = \iiint_V {}_B\Phi_AI_VdV - \iiint_V {}_A\Phi_BI_VdV \tag{19}$$

independent of the conductivity, or

$$\iint_S {}_A\Phi_BK^in_idS + \iiint_V {}_A\Phi_BI_VdV = \iint_S {}_B\Phi_AK^in_idS + \iiint_V {}_B\Phi_AI_VdV. \tag{20}$$

Appendix II

Solution to the Problem of Three Concentric Spheres with Point Electrodes on the Surface

A solution to Laplace's equation appropriate to this problem in each of the three conducting regions is

$$\Phi(r,\theta,\phi) = \sum_{n=0}^{\infty}\sum_{m=0}^{n} A_m\cos m\phi(B_nr^n + C_nr^{-(n+1)})P_n{}^m(\cos\theta). \tag{21}$$

$\Phi(r,\theta,\phi)$ is the potential expressed as a function of the spherical coordinates r, θ, and ϕ. $P_n{}^m(\cos\theta)$ is the associated Legendre polynomial of the first kind, and the subscripted constants A_m, B_n, and C_n are to be determined

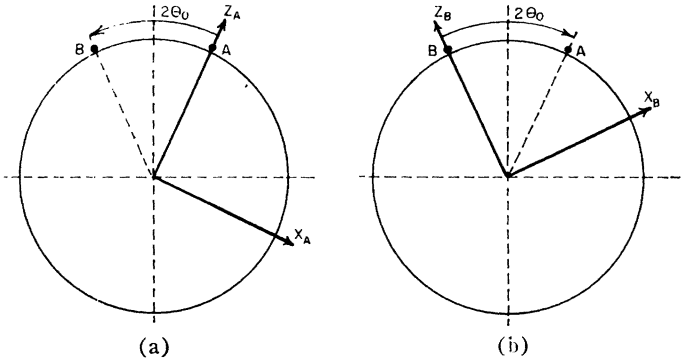

Fig. 6. Geometry for the coordinate transformation. (a) Coordinates for electrode A calculations. (b) Coordinates for electrode B calculations.

from the boundary conditions. The coordinates and geometry shown in Fig. 5 can always be arranged for any arbitrary electrode placement on the sphere surface.

Matching boundary conditions at $r=a$ and $r=b$ where the potentials and normal current densities are continuous follows the standard procedure. On the outer surface the potential becomes singular at the electrodes; a method for satisfying conditions at the boundary can be found in Smythe [12].

Using biaxial harmonics [13] the solution can be separated into two parts having the azimuthal symmetry shown in Fig. 6. This is an important simplification since the double summation in associated Legendre polynomials is reduced to two single summations in ordinary Legendre polynomials. The following results can then be obtained for the potentials Φ_b, Φ_s, and Φ_t in the brain, skull, and scalp tissue, respectively:

$$\Phi_b = \frac{I}{2\pi\sigma_t c}\sum_{n=1}^{\infty} A_n\left(\frac{r}{c}\right)^n [P_n(\cos\theta_A) - P_n(\cos\theta_B)] \tag{22}$$

$$\Phi_s = \frac{I}{2\pi\sigma_t c}\sum_{n=1}^{\infty} [S_n r^n + U_n r^{-(n+1)}] \cdot [P_n(\cos\theta_A) - P_n(\cos\theta_B)] \tag{23}$$

$$\Phi_t = \frac{I}{2\pi\sigma_t c}\sum_{n=1}^{\infty} [T_n r^n + W_n r^{-(n+1)}] \cdot [P_n(\cos\theta_A) - P_n(\cos\theta_B)]. \tag{24}$$

The two parts of each expression in effect display the potential from each electrode (designated by the subscripts A and B) separately. The coefficients are found to be

$$A_n = \frac{(2n+1)^3/2n}{\left\{\left[\left(\frac{\sigma_b}{\sigma_s}+1\right)n+1\right]\left[\left(\frac{\sigma_s}{\sigma_t}+1\right)n+1\right] + \left(\frac{\sigma_b}{\sigma_s}-1\right)\left(\frac{\sigma_s}{\sigma_t}-1\right)n(n+1)\left(\frac{a}{b}\right)^{2n+1} + \left(\frac{\sigma_s}{\sigma_t}-1\right)(n+1)\left[\left(\frac{\sigma_b}{\sigma_s}+1\right)n+1\right]\left(\frac{b}{c}\right)^{2n+1} + \left(\frac{\sigma_b}{\sigma_s}-1\right)(n+1)\left[\left(\frac{\sigma_s}{\sigma_t}+1\right)(n+1)-1\right]\left(\frac{a}{c}\right)^{2n+1}\right\}} \tag{25}$$

(where σ_b, σ_s, and σ_t are the conductivities of the three regions)

$$S_n = \frac{\frac{A_n}{c^n}\left[\left(1-\frac{\sigma_b}{\sigma_s}\right)n+1\right]}{2n+1} \tag{26}$$

$$U_n = \frac{\frac{A_n}{c^n}n\left(1-\frac{\sigma_b}{\sigma_s}\right)a^{2n+1}}{2n+1} \tag{27}$$

$$T_n = \frac{A_n}{c^n(2n+1)^2}\left\{\left[\left(1+\frac{\sigma_b}{\sigma_s}\right)n+1\right]\left[\left(1+\frac{\sigma_s}{\sigma_t}\right)n+1\right]+n(n+1)\left(1-\frac{\sigma_b}{\sigma_s}\right)\left(1-\frac{\sigma_s}{\sigma_t}\right)\left(\frac{a}{b}\right)^{2n+1}\right\} \tag{28}$$

$$W_n = \frac{nA_n}{c^n(2n+1)^2}\left\{\left(1-\frac{\sigma_s}{\sigma_t}\right)\left[\left(1+\frac{\sigma_b}{\sigma_s}\right)n+1\right]b^{2n+1}+\left(1-\frac{\sigma_b}{\sigma_s}\right)\left[\left(1+\frac{\sigma_s}{\sigma_t}\right)n+\frac{\sigma_s}{\sigma_t}\right]a^{2n+1}\right\} \tag{29}$$

The current density in each region can be found by taking the negative gradient of the potential and multiplying by the conductivities appropriate to the region. For polar electrode locations, the current density at the origin is

$$J_b = J_{bA} + J_{bB} = \frac{-I\sigma_b}{\pi\sigma_t c^2}A_1. \tag{30}$$

References

[1] S. Rush and D. A. Driscoll, "Current distribution in the brain from surface electrodes," *Anesthesia and Analgesia*, vol. 47, pp. 717–723, November–December 1968.

[2] M. A. B. Brazier, "The electrical fields at the surface of the head during sleep," *Electroencephalog. Clin. Neurophysiol.*, vol. 1, pp. 195–204, 1949.

[3] C. D. Geisler and G. L. Gerstein, "The surface EEG in relation to its sources," *Electroencephalog. Clin. Neurophysiol.*, vol. 13, pp. 927–934, 1961.

[4] P. L. Paicer, A. Sances, and S. J. Larson, "Theoretical evaluation of cerebral evoked potentials," *Proc. 20th ACEMB* (Boston, Mass.), paper 14.1, 1967.

[5] H. Helmholtz, "Über einige Gesetz der Vertheilung elektrischer Ströme in körperlichen Leitern, mit Anwendung auf die thierisch-elektrischen Versuche," *Ann. Phys. Chem.*, ser. 3, vol. 29, pp. 211–233 and 353–377, 1853.

[6] R. McFee and F. D. Johnston, "Electrocardiographic leads, I," *Circulation*, vol. 8, pp. 554–568, October 1953; pt. II, vol. 9, pp. 255–266, February 1954; pt. III, vol. 9, pp. 868–880, June 1954.

[7] D. A. Brody and W. E. Romans, "A model which demonstrates the quantitative relationship between the electromotive forces of the heart and the extremity leads," *Am. Heart J.*, vol. 45, pp. 253–266, 1953.

[8] D. A. Brody, J. C. Bradshaw, and J. W. Evans, "A theoretical basis for determining heart-lead relationships of the equivalent cardiac multipole," *IRE Trans. Bio-Medical Electronics*, vol. BME-8, pp. 139–143, April 1961.

[9] R. Plonsey, "Reciprocity applied to volume conductors and the ECG," *IEEE Trans. Bio-Medical Electronics*, vol. BME-10, pp. 9–12, January 1963.

[10] P. W. Nicholson, "Specific impedance of cerebral white matter," *Exptl. Neurol.*, vol. 13, pp. 386–401, 1965.

[11] R. McFee and S. Rush, "Qualitative effects of thoracic resistivity variations on the interpretation of electrocardiograms: The 'Brody' effect," *Am. Heart J.*, vol. 74, pp. 642–651, November 1967.

[12] W. R. Smythe, *Static and Dynamic Electricity*. New York: McGraw-Hill, 1950, p. 239.

[13] *Ibid*,. p. 154, eq. (5).

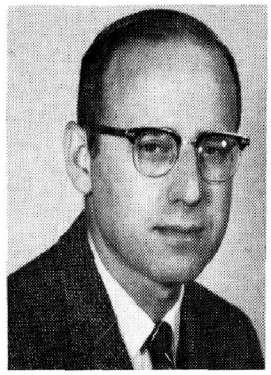

Stanley Rush (SM'53) was born in Brooklyn, N. Y., on June 17, 1920. He received the B.S. degree in physics from Brooklyn College, Brooklyn, N. Y., in 1942, and the M.S. degree in electrical engineering and the Ph.D. degree both from Syracuse University, Syracuse, N. Y., in 1958 and 1962, respectively.

In 1942 he joined the U. S. Army Signal Corps as a Radar Officer; in that capacity he completed the radar training programs at Harvard University and M.I.T., Cambridge, Mass., and served overseas with the Ninth Air Force for two years. In 1946, as a civilian, he was employed as a Design and Development Engineer on direction finding apparatus at the RCA Victor Division, Camden, N. J. In 1947 he joined the USAF Watson Laboratories, Eatontown, N. J., which later became the Rome Air Development Center, Griffiss AFB, N. Y. As electronic engineer and scientist with these organizations, he worked on the development of automatic tracking equipment and related components for ground-controlled approach radars, and eventually was responsible for systems studies and supporting research for radar defenses against ballistic missiles. He was Project Engineer on the initial studies that led to the BMEWS network and Chief of the Ballistic Missile Support Laboratory until 1957. He has been an Instructor in electrical engineering at Syracuse University and is now a Professor in the Electrical Engineering Department of the University of Vermont, Burlington. His present research interests include electromagnetic fields, electrocardiography, electrophysiology, and electronarcosis.

Dr. Rush is a member of the New York Academy of Sciences and Sigma Xi.

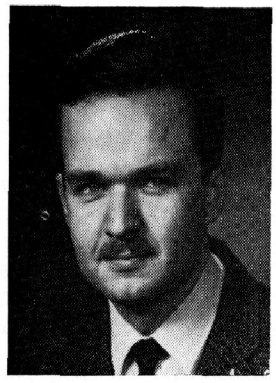

Daniel A. Driscoll (S'68) was born in Brooklyn, N. Y. He received the E.E. degree from the University of Cincinnati, Cincinnati, Ohio, and the M.E.E. degree from Renssalaer Polytechnic Institute, Troy, N. Y.

He was a part of cooperative education at Baldwin Piano Company while at Cincinnati, and is interested in musical acoustics, having recently published a paper on the acoustical characteristics of the recorder. In 1964, he was appointed Assistant Professor of Electrical Engineering at Union College, Schenectady, N. Y. He is presently on leave from Union College while completing studies for the Ph.D. degree in bio-medical engineering at the University of Vermont, Burlington. He is engaged in research studying the path of current applied to scalp electrodes in the human brain. Applications include electroanesthesia and the interpretation of electroencephalograms.

Mr. Driscoll is a member of the American Society of University Professors, the American Society for Engineering Education, Tau Beta Pi, Eta Kappa Nu, and Sigma Xi.